**IEEE** *Access*

# Simulation of Influence of DC Pre-Stress on Space-Charge Characteristics of Cross-Linked Polyethylene in Inhomogeneous Field

HECHEN LIU[ID][1], XIAOBIN XU[ID][1], YUN-PENG LIU[1,2], (Member, IEEE), SHAOXIN MENG[3], ZHANPENG GUO[1], AND MINGJIA ZHANG[1]

[1]Hebei Provincial Key Laboratory of Power Transmission Equipment Security Defense, North China Electric Power University, Baoding 071003, China
[2]State Key Laboratory of Alternate Electrical Power System With Renewable Energy Sources, North China Electric Power University, Beijing 102206, China
[3]State Key Laboratory of Power Grid Environmental Protection, China Electric Power Research Institute, Wuhan 430074, China

Corresponding author: Xiaobin Xu (281659683@qq.com)

**ABSTRACT** Space charge is one of the main causes of electrical tree initiation in high-voltage cable insulation. To investigate the influence of DC pre-stress on the space-charge distribution of cross-linked polyethylene (XLPE), a two-dimensional needle-plate electrode model is established in this study. Based on the bipolar charge-transport model, the space-charge distribution characteristics of the needle-plate electrode model under DC pre-stress are simulated and analyzed. The space-charge distribution characteristics are compared with that of the grounded DC electrical tree initiation properties. The work in this study illustrates that the pre-stress time and value affect the space-charge distribution characteristics. There is a certain relationship between space-charge distribution characteristics and electrical tree initiation characteristics. The distribution range of the DC grounded electrical tree is very similar to that of space charge. Both have a similar distribution shape and increased trend under different pre-stress times, and both have an obvious polarity effect.

**INDEX TERMS** DC pre-stress, grounded electrical tree, space charge simulation, XLPE.

## I. INTRODUCTION

With the rapid development of high-voltage direct-current (HVDC) transmission, cross-linked polyethylene (XLPE) cable has been widely used in new energy transmission, submarine cable transmission, and other fields because of its excellent electrical insulation performance and simple construction technology [1].

Relevant studies have shown that the formation and development of an electrical tree are the symptoms of cable insulation deterioration, which seriously affects the safe and stable operation of cables, and the accumulation of space charge is the main cause of electrical treeing [2]. When space charge is injected into the insulation material, the local electric field will change. When the local electric field intensity is too high, the insulation will deteriorate or even break down, forming a dendritic discharge channel. The continuous development of

The associate editor coordinating the review of this manuscript and approving it for publication was George Chen.

an electrical tree can be considered as the process of space charge penetrating into the dielectric along the tip of the tree [3]–[5]. The influence mechanism of space charge on an electrical tree is complicated. At present, the commonly used theories are space-charge injection extraction theory, electroluminescence theory, and thermal electron theory, among others [6]–[8].

At present, a significant amount of research has been done on the space-charge distribution characteristics under DC voltage. It is generally believed that a large number of homo-polar space charges will be injected into the insulation under DC pre-stress to form a space-charge shielding layer. Regarding extremely inhomogeneous electric fields, such as needle-plate electrode systems, space charges of the same polarity will homogenize the electric field at the tip of the needle, resulting in a significant increase of electrical tree initiation voltage [9], [10]. However, once stimulated by the surrounding environment, such as temperature increase, radiation, and sudden short-circuit grounding of the needle

**IEEE** *Access*

H. Liu *et al.*: Simulation of Influence of DC Pre-Stress on Space-Charge Characteristics of XLPE in Inhomogeneous Field

tip, the trapped space charge will de-trap quickly, releasing a large amount of mechanical electrical energy, and even lead to material breakdown [11]. The polarization charge transport-model proposed by Baudoin can well explain the process of space-charge generation, transmission, trapping, and recombination in a polymer under the action of steady-state uniform electric field [12]. Liu *et al.* studied the initiation characteristics of the electrical tree under DC-impulse voltage [13]. They believed that when the impulse voltage acts, the steady-state space charge will be de-trapped and its movement will be accelerated, resulting in the instantaneous breakage of the molecular chain of the material at the tip of the needle, and then the electrical tree is initiated. Wang *et al.* used the bipolar charge-transport model to simulate and analyze the space-charge distribution characteristics in samples under DC pre-stress at different temperatures [14]. They pointed out that the space-charge behavior under DC pre-stress was closely related to the initiation and growth characteristics of a DC-grounded electrical tree. Zhang *et al.* used the pressure-wave propagation method to study the space-charge distribution characteristics in polyethylene with different insulation thicknesses [15]. The results show that the insulation thickness is the main factor affecting the space-charge characteristics.

When defects exist in DC cable, the extremely uneven field near the defects will affect the space-charge distribution characteristics, and then affect the electrical tree characteristics under DC voltage. At present, there are few studies on the influence of space-charge distribution in XLPE under DC pre-stress in extremely uneven fields, and the mechanism of the influence of space-charge distribution on DC electrical tree initiation is not clear. Based on the bipolar charge-transport model, a two-dimensional sample model with needle inside was set up, and the space-charge distribution characteristics of samples at $\pm20$, $\pm40$ and $\pm50$ kV under different pre-stress times were simulated. In this study, the influence of pre-stress time of DC voltage on the space-charge distribution characteristics under an extremely inhomogeneous field was investigated, and the space-charge distribution characteristics were compared with the initiation characteristics of grounded electrical trees.

## II. SPACE-CHARGE SIMULATION
### A. BIPOLAR CHARGE-TRANSPORT MODEL
The bipolar charge-transport model considers that there exists an obvious bipolarity for the transport of charge, and the electrons and holes injected from the electrode are the main source of carriers [16]. The principle of the model is shown in Fig. 1. The model assumes that the charge sources are the electrons and holes injected by the electrodes, and the modulation effect of shallow traps on charge-carrier mobility is characterized by effective mobility $\mu$. The deep traps are simplified to a single level, and the trapping process of electrons and holes are characterized by trapping coefficients $B_e$ and $B_h$, respectively. The recombination
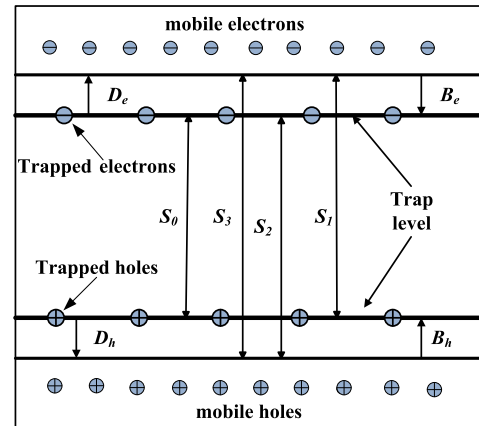


**FIGURE 1.** Schematic of bipolar charge transport model.

phenomena of charge carriers are characterized by recombination coefficients $S_0$, $S_1$, $S_2$ and $S_3$. The conduction process of the bipolar charge-transport model consists of four parts: injection of electrons and holes from the electrodes, trapping, de-trapping, and recombination. The injection of electrons and holes follows the Schottky injection mode [14], and the injection equations are expressed as follows:

$$j_e(0,t) = AT^2 \exp\left(-\frac{w_{ei}}{KT}\right) \exp\left(\frac{e}{KT}\sqrt{\frac{eE(0,t)}{4\pi\varepsilon}}\right) \quad (1)$$

$$j_h(d,t) = AT^2 \exp\left(-\frac{w_{hi}}{KT}\right) \exp\left(\frac{e}{KT}\sqrt{\frac{eE(d,t)}{4\pi\varepsilon}}\right) \quad (2)$$

where subscripts $h$ and $e$ indicate holes and electrons, respectively; $A$ is the Richardson constant, 600 m$^2$/C/s; $w_{ei}$ and $w_{hi}$ represent the injection barriers between electrode and insulating material, in eV, respectively; $j$ denotes the current densities; $E$ denotes the electric field intensity, in V/m; $K$ is Boltzmann's constant; $T$ is the insulating temperature, in K; $e$ is the elementary charge; and $\varepsilon$ is the permittivity of the insulation material.

In the material, the transport process of injected charge carriers can be expressed by a conservative equation, transport equation, and Poisson's equation, respectively, as follows:

$$\frac{\partial n_a(x,t)}{\partial t} + \frac{\partial j_a(x,t)}{\partial x} = s_a(x,t) \quad (3)$$

$$j_a(x,t) = \mu_a n_a E(x,t) \quad (4)$$

$$\frac{\partial E(x,t)}{\partial x} = \frac{n_e + n_h}{\varepsilon_r + \varepsilon_0} \quad (5)$$

where subscript $a$ represents the type of the charges; $n_a$ denotes the density of carriers; $j_a$ are the current densities; $\varepsilon_0$ and $\varepsilon_r$ are the permittivities of the vacuum and dielectric constant, respectively; $s_a$ is the source term, including $s_{eu}$, $s_{et}$,

H. Liu *et al.*: Simulation of Influence of DC Pre-Stress on Space-Charge Characteristics of XLPE in Inhomogeneous Field

**IEEE** *Access*

$s_{hu}$ and $s_{ht}$; and $\mu$ is the effective mobility:

$$
\begin{cases}
s_{eu} = -S_1 \cdot n_{ht} \cdot n_{eu} - S_3 \cdot n_{hu} \cdot n_{eu} - \\
\quad B_e \cdot n_{eu} \cdot \left(1 - \frac{n_{et}}{n_{oet}}\right) + D_e \cdot n_{et} \\
s_{et} = -S_2 \cdot n_{hu} \cdot n_{et} - S_0 \cdot n_{ht} \cdot n_{et} + \\
\quad B_e \cdot n_{eu} \cdot \left(1 - \frac{n_{et}}{n_{oet}}\right) + D_e \cdot n_{et} \\
s_{hu} = -S_2 \cdot n_{hu} \cdot n_{et} - S_3 \cdot n_{hu} \cdot n_{eu} - \\
\quad B_h \cdot n_{hu} \cdot \left(1 - \frac{n_{ht}}{n_{oht}}\right) + D_h \cdot n_{ht} \\
s_{ht} = -S_1 \cdot n_{ht} \cdot n_{eu} - S_0 \cdot n_{ht} \cdot n_{et} + \\
\quad B_h \cdot n_{hu} \cdot \left(1 - \frac{n_{ht}}{n_{oht}}\right) + D_h \cdot n_{ht}
\end{cases}
\tag{6}
$$

In (6), $S_0$, $S_1$, $S_2$, and $S_3$ are the coefficients of recombination; $B_e$ and $B_h$ are the trapping coefficients of electrons and holes, respectively; $n_{oet}$ and $n_{oht}$ are the densities of deep traps for electrons and holes, respectively, $D_e$ and $D_h$ are the de-trapping coefficients for trapped electrons and holes, respectively; and subscripts *eu*, *et*, *hu* and *ht* represent mobile electrons, trapped electrons, mobile holes, and trapped holes, respectively.

## B. ESTABLISHMENT AND SOLUTION OF MODEL

The bipolar charge-transport model has been widely used to analyze the space-charge distribution under flat electrodes. A one-dimensional model is not applicable to the problem of space-charge distribution under a non-uniform electric field. Therefore, a two-dimensional model of a needle-plane electrode is established in this paper, and the influence of DC voltage on space-charge distribution is analyzed based on the bipolar charge-transport model. The curvature radius of the needle electrode is 3 $\mu$m, the cone angle of the needle tip 30°, and the distance between the needle tip and plane electrode 2 mm. The DC voltages applied onto the needle electrode are ±20, ±40, and ±50 kV, and the voltage boost rate is 2 kV/s in the simulation. The plane electrode is grounded reliably. The transient solution is used to simulate and analyze the distribution of space charge in 3,600 s. The solution is divided into two parts: one is the distribution of electric field affected by space charge, and the other is the distribution of space charge under the electric field. The boundary injection of space charge satisfies (1) and (2), the charge-transfer process satisfies (3)–(5), and the charge density change of the non-conduction process satisfies (6). Values of the material parameters needed in the simulations were chosen in accordance with [14], [17], and [18]. The values of the material parameters are displayed in Table 1. The simulation was completed using COMSOL Multiphysics®.

## III. SIMULATION RESULTS

The space-charge density from the tip of the needle to the plane electrode was extracted as shown in Fig. 2. Fig. 2 (a)-(c) shows the space-charge densities at different locations of the sample at DC pre-stress amplitudes of ±50, ±40, and ±20 kV, respectively. The origin of abscissa in Figs. 2 is the position of needle tip. Make a vertical line from the needle tip to the flat electrode, and the distance

**TABLE 1.** Parameter settings of simulation process.

| Symbol | Value | Units | Description |
|---|---|---|---|
| $w_{ei}$ | 1.3 | eV | Injection barrier |
| $w_{hi}$ | 1.35 | eV | Injection barrier |
| K | $1.38\times10^{-23}$ | J/K | Boltzmann's constant |
| $S_0$-$S_2$ | $4\times10$-3 | m²/C/s | Recombination coefficients |
| $S_3$ | 0 | mA×(mm²×K²) | Recombination coefficients |
| A | 600 | m²/C/s | Richardson constant |
| $\mu_e$ | $1.0\times10^{-13}$ | s·mol/kg | Effective mobility |
| $\mu_h$ | $8.3\times10^{-14}$ | s·mol/kg | Effective mobility |
| T | 303 | K | Temperature |
| $B_e$ | 0.1 | 1/s | Trapping coefficient |
| $B_h$ | 0.1 | 1/s | Trapping coefficient |
| $n_{oht}$ | 100 | C/m³ | Densities of deep traps |
| $n_{oet}$ | 100 | C/m³ | Densities of deep traps |
| $D_e$ | $6.35\times10^{-4}$ | 1/s | De-trapping coefficient |
| $D_h$ | $2.01\times10^{-4}$ | 1/s | De-trapping coefficient |

from the vertical line to the needle tip is the abscissa value. In Figs. 2, Fig. 3 and Fig. 7, space charges are homo-polar charges. It can be seen from Figs. 2 and 3 that the distribution of space charge under DC pre-stress has an obvious polarity effect, and the space-charge density and charge injection depth under the positive polarity are smaller than those under the negative. The space-charge density and charge injection depth increase with the increasing pre-stress time under positive and negative DC voltages, but the growth rate gradually slows and shows a significant saturation trend. The farther away from the needle electrode, the lower the space-charge density. Compared with (a), (b) and (c) in Figs. 2, it can be seen that the space-charge density and injection depth increase with increasing DC pre-stress amplitude. The space charge density and injection depth are the largest at ±50 kV and the smallest at ±20 kV.

As shown in Figs. 2(a) and 3, when the DC pre-stress value is ±50 kV, the space-charge density at the tip of the needle increase with the pre-stress time, but the density increasing trend slows gradually, until finally becoming saturated. When a DC pre-stress is applied, the homo-polar space charge is continuously injected into the tip of the needle, and the density and distribution range of the charges gradually increase over time. Most of the charges are trapped near the tip, forming a space-charge layer, which can form a counter electric field. The counter electric field weakens the electric field intensity near the tip of the needle, which leads to the limitation of space-charge accumulation and diffusion. In addition, the counter electric field prevents the further injection of space charge to a certain extent. With increasing space-charge density, the electric field intensity of the counter electric field increases gradually, and the inhibition ability of the charge injection increases gradually, which leads to the decrease in the growth rate of the space-charge density and finally to saturation. The space charge saturates in different degrees under the DC pre-stress of positive and negative polarity, but the charge saturates more easily in negative polarity than in positive polarity. The saturation of space charge under
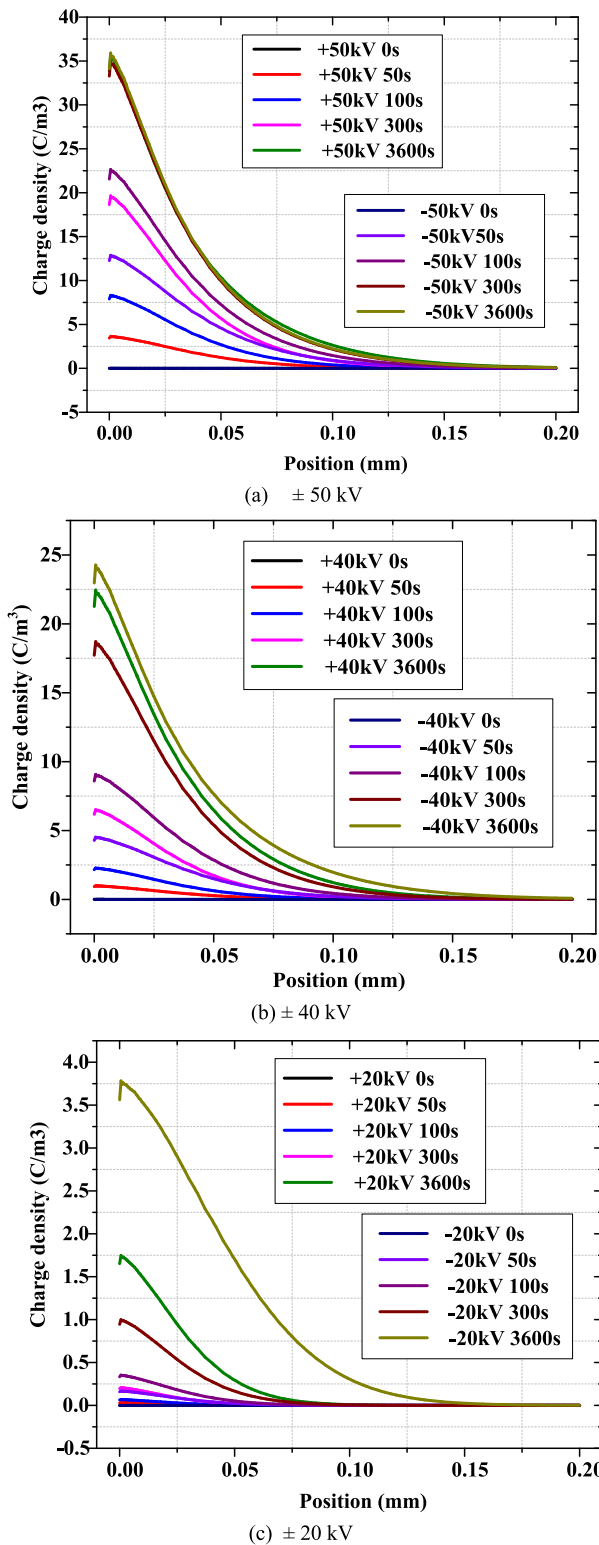
**IEEE** *Access*

H. Liu *et al.*: Simulation of Influence of DC Pre-Stress on Space-Charge Characteristics of XLPE in Inhomogeneous Field



(a) ± 50 kV



(b) ± 40 kV



(c) ± 20 kV

**FIGURE 2.** Simulation results of space charge density at each position.



**FIGURE 3.** Variations in the maximum density of space charge at the needle tip with time under different voltages.

density is larger and easier to reach saturation and the space-charge injection depth is deeper under the negative DC pre-stress. The difference in space-charge distribution between positive and negative polarity may be caused by the difference of electron and hole motion characteristics. Compared with holes, electrons are easier to inject into the medium, and the volume of the electrons is smaller, the average free path larger, and the mobility stronger [20]. Therefore, under negative DC pre-stress, the space-charge injection depth is deeper and the space-charge density larger.

Fig.3 shows the maximum space charge density at the needle tip under different voltages. As can be seen from Figs. 2 and 3, when the pre-stress values are ±50, ±40, and ±20 kV, the space-charge density and distribution range are sequentially decreased under the same pre-stress time, and the higher the voltage, the higher the space-charge increase rate. The simulation results show that under DC pre-stress, a large number of homopolar space charges are injected into the insulation and thus accumulate near the tip. Most of the space charges are trapped near the tip. When the pre-stress value is high, the electric field near the needle electrode is high, which easily leads to a large number of charge-carrier injections. Therefore, when the pre-stress time is the same, the space-charge density and distribution range at the needle electrode increase significantly with increasing pre-stress DC voltage.

To further explore the influence of space-charge injection, migration, and diffusion on the electric field intensity, the electric field intensities under various voltages are shown in Fig. 4. When DC pre-stress time is 1,200 s, the charge basically reaches the steady-state distribution, and the electric field intensity is similar to 3,600 s. Therefore, Fig. 4 compares and analyzes the change of electric field intensity when DC pre-stress time is 0s and 1200s under different voltages. Fig. 4 shows that the electric field intensity at 1,200 s is obviously smaller than that at 0 s. As can be seen in the

negative DC pre-stress is easier to achieve than that under positive DC pre-stress, which is related to the difference of electron and hole motion.

As shown in Figs. 2(a) and 3, the distribution of space charges has an obvious polarity effect. The space-charge
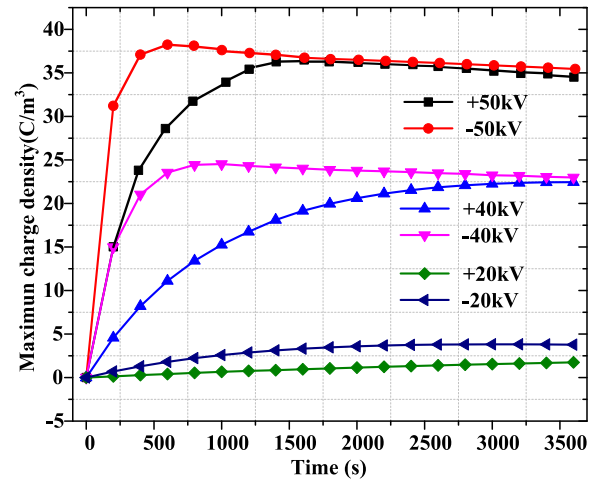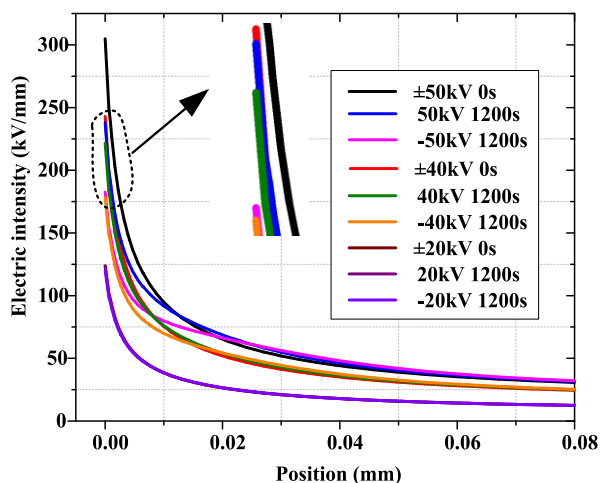
H. Liu *et al.*: Simulation of Influence of DC Pre-Stress on Space-Charge Characteristics of XLPE in Inhomogeneous Field

IEEE *Access*



**FIGURE 4.** Distribution of electric field intensity with position near needle tip under different voltages.



**FIGURE 5.** Relation between the grounded dc tree length and different pre-stress times [19].

figure, the electric field intensity at the tip of the needle decreases with increasing DC pre-stress time under positive and negative polarity DC voltage, and the higher the DC pre-stress voltage, the greater the decrease of electric field intensity. In addition, the electric field intensity of negative DC voltage is significantly lower than that of positive DC voltage. Studies have shown that space charge can effectively improve the internal electric field distribution of the sample and homogenize the electric field intensity. It can be seen from Figs.2 and 3 that under positive and negative DC voltages, with increasing DC pre-stress time and amplitude, the space-charge density gradually increases. Therefore, the degree of homogeneity of the electric field is gradually strengthened by the homo-polar space charges, which makes the electric field intensity decrease with increasing DC pre-stress time and amplitude. In the same way, the electric field intensity of the negative DC voltage is less than that of the positive one, which is caused by the difference in the uniformity of space charge to the electric field intensity.

## IV. ANALYSIS AND DISCUSSION

To analyze the influence of space-charge accumulation on the initiation characteristics of electrical trees, the simulation results are compared with the grounded DC tree initiation properties that are based on the grounded DC tree tests conducted by our research team. Fig. 5 shows the influence of DC pre-stress voltage on the initiation length of the grounded DC trees [19]. The experimental methods details were discussed in [19] and [20]. The DC pre-stress values are ±20, ±22.5, ±40, and ±50 kV and the DC pre-stress times 10 s, 5 min, and 1 h.

As shown in Fig. 5, the initiated electrical tree length becomes longer with longer pre-stress times. Moreover, when the pre-stress amplitude and time are the same, the electrical tree initiation length under negative DC voltage is significantly longer than that of a positive one. Besides, when the
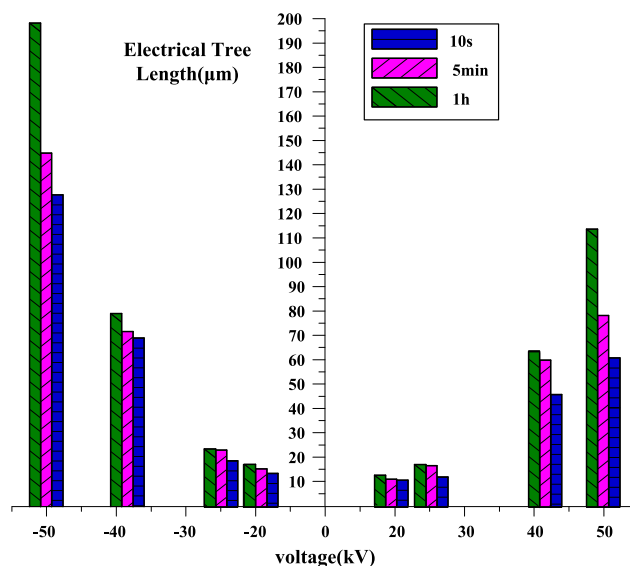
pre-stress DC voltage is larger, the electrical tree initiation length increase trend is greater. This trend is quite similar to that of space charge shown in Fig. 3, indicating that there may be a relationship between the space charge and initiation properties of the grounded DC tree.

To investigate this relationship, the electrical tree distribution characteristics are compared with those of the space charge. As the randomness of the initiation characteristics of the electrical tree is quite large, a single electrical tree cannot reflect the distribution range of the electrical tree. Therefore, a set of DC grounded electrical trees (more than 30 samples) are superimposed, as shown in Fig. 6. To some extent, this can reflect the distribution range of the DC grounded electrical tree. Then, the simulated distributions of space charge near the needle tip under DC pre-stress are compared with the distribution of the electrical trees. Due to the length of the manuscript, only 10 s and 5 min of pre-stress times with pre-stress voltages of ±40 and +50 kV are shown in Fig.6. A dotted line is used to represent the distribution range of the electrical trees. Fig.7 shows the simulated space-charge distribution under the same voltage and pre-stress time. The influence of pre-stress time on the electrical tree distribution range can be obtained by comparing the electrical tree stacking chart under the DC pre-stress time of 10 s and 5 min. The influence of voltage polarity on the electrical tree distribution range can be known by comparing the electrical tree stacking chart under ±40 kV DC pre-stress. The influence of DC pre-stress amplitude on the electrical tree distribution range can be obtained by comparing the electrical tree stacking chart under +40 kV and +50 kV DC pre-stress. The abscissa and ordinate in Fig. 7 represent the geometric distance from the needle tip; that is, the needle tip is taken as the origin, and the units of the abscissa and ordinate are millimeters. Comparing Fig. 6 with Fig. 7, we can find that the distribution
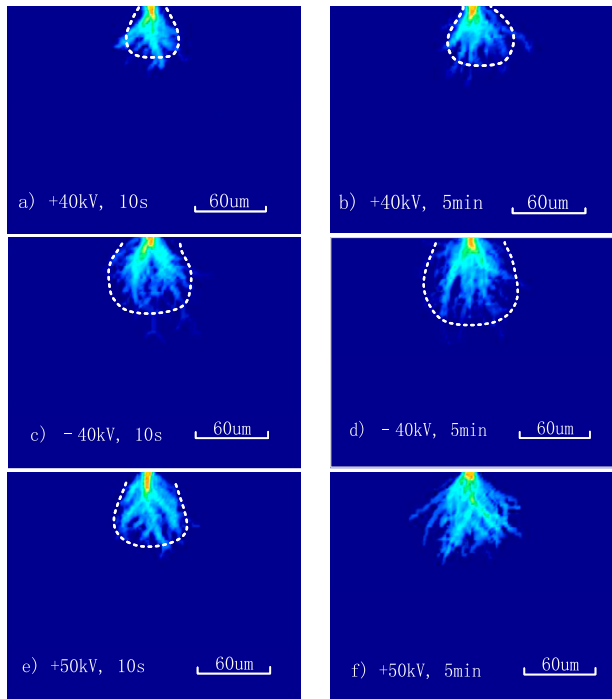
**IEEE** *Access*

H. Liu *et al.*: Simulation of Influence of DC Pre-Stress on Space-Charge Characteristics of XLPE in Inhomogeneous Field



**FIGURE 6.** Electrical tree stacking chart.



**FIGURE 7.** Simulated space-charge results. (The abscissa and ordinate represent the geometric distance from the needle tip; that is, the needle tip is taken as the origin; and the units of the abscissa and ordinate are mm.)



**FIGURE 8.** Variation of tree length and maximum space-charge depth at defects with time at ±40 kV.

range of the DC grounded electrical tree is very similar to that of space charge. Both have a similar distribution shape and increase trend under different pre-stress times. Therefore, the distribution characteristics of the DC grounded tree may be used to qualitatively analyze the space charge distribution near the needle tip under DC voltage.

To further determine the relationship discussed above, the relationship of the length of DC-grounded electrical tree, and the injection depth of simulated space charge was analyzed, as shown in Fig. 8. In the calculation of space-charge injection depth in Fig. 8, the charge-density threshold is 0.7 C/m$^3$. It can be seen from the figure that the increase trends of the two parameters were quite similar; that is, at the beginning, both parameters increase rapidly, and then the increase trend slowed and gradually saturated. These results show that there is a certain relationship between the space-charge injection depth and length of the electrical tree. References [21] and [22] show that space-charge injection depth can effectively affect the electrical tree initiation length. However, the qualitative relationship between the space charge characteristics and the electrical tree characteristics is not given in this paper. The quantitative relationship and theoretical analysis between the two is also a direction worth exploring in the future.

When DC voltage is applied, a large number of homo-polar charges are rapidly injected into the material from the needle tip. Some of the charges are trapped by the shallow traps near the tip. Because the energy level of the shallow traps is small, the charges de-trap and continue to move towards the interior of the medium. Some of the charges are trapped
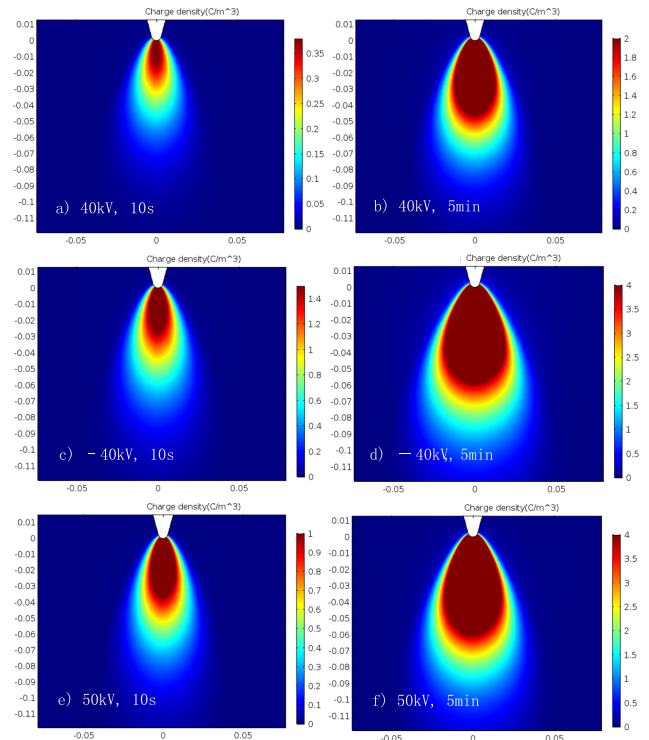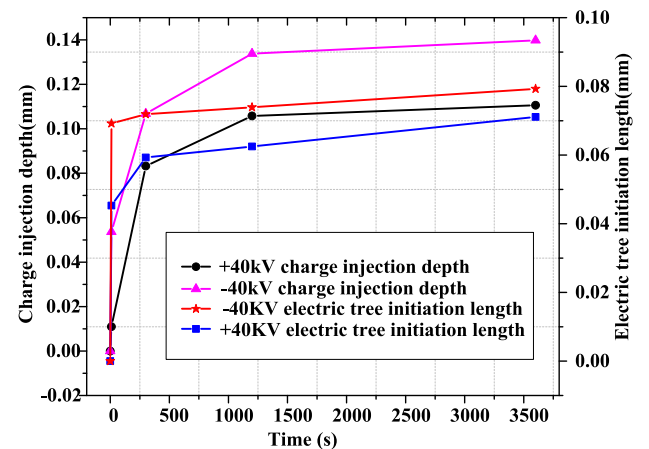
by the deep traps in the medium. Because of the high energy level of the deep traps, the trapped charges are difficult to de-trap, so the space charges are accumulated in the medium. The accumulated space charge forms a space-charge layer. Since the electric field intensity at the tip of the needle is weakened by the space-charge layer, the further diffusion and accumulation of space charge are limited, so the space-charge density shows a significant saturation trend with increasing pre-stress time. At the same time, the injected space charge will form

H. Liu *et al.*: Simulation of Influence of DC Pre-Stress on Space-Charge Characteristics of XLPE in Inhomogeneous Field

IEEE *Access*

a counter electric field on the electrode. With increasing space-charge density, the electric field intensity of the counter electric field will increase gradually, which restrains the space charge injection and makes the space-charge injection rate decrease gradually with increasing time and finally reach equilibrium. Once the needle tip is stimulated by external factors, such as a sudden short-circuit, the trapped charge will quickly de-trap and release a significant amount of energy. If the energy is high enough, the molecular structure of the material near the needle tip will be destroyed, forming an electrical tree discharge channel [10]. According to space-charge injection-extraction theory [20], in the DC pre-stress stage the amount, injection depth, distribution range, and other factors of the space charge accumulated at the front of the needle tip will directly affect the process of space-charge de-trapping after the needle tip is stimulated by the external environment. As the pre-stress time increases, the space charge migrates and diffuses continuously, which leads to the differences in the length and shape of the initiation of the electrical tree.

## V. CONCLUSIONS
Based on a simulation study, the influence of DC pre-stress on space-charge characteristics is analyzed in this study. In addition, the relationship between the length of the grounded DC tree and space-charge distribution under different DC pre-stress voltages and times is further revealed. The relevant research conclusions are the following:

1) The pre-stress time and value affect the space-charge distribution characteristics. When the DC pre-stress voltage is applied, the amount of space charge near the needle electrode and the range of charge distribution increase slightly with increasing pre-stress time, but the increase trend gradually decreases and shows a significant saturation trend.

2) The distribution of space charge has an obvious polarity effect. When the pre-stress time and amplitude are the same, the space-charge density and distribution range of negative DC pre-stress are larger than those of positive DC pre-stress, and the charge is more easily saturated under the negative polarity.

3) A relationship exists between space-charge distribution characteristics and electrical tree initiation characteristics. The distribution range of the DC grounded electrical tree is very similar to that of space charge. Both have a similar distribution shape and an increase trend under different pre-stress times. Therefore, it is believed that the electrical tree initiation length can be influenced by the space charge density and injection depth.

4) When space charge is difficult to measure, the distribution of the electrical tree can be used to approximately evaluate the space charge distribution characteristics.

## REFERENCES
[1] Y. Zhou, Y. Zhang, L. Zhang, D. Guo, X. Zhang, and M. Wang, "Electrical tree initiation of silicone rubber after thermal aging," *IEEE Trans. Dielectr. Electr. Insul.*, vol. 23, no. 2, pp. 748–756, Apr. 2016.

[2] Y. Zheng, Y. V. Serdyuk, and S. M. Gubanski, "Space charge controlled electric field preceding inception of electric tree in XLPE at AC voltage," in *Proc. IEEE 11th Int. Conf. Properties Appl. Dielectric Mater. (ICPADM)*, Sydney, NSW, Australia, Jul. 2015, pp. 132–135.

[3] L. Ying and C. Xiaolong, "Electrical tree initiation in XLPE cable insulation by application of DC and impulse voltage," *IEEE Trans. Dielectr. Electr. Insul.*, vol. 20, no. 5, pp. 1691–1698, Oct. 2013.

[4] I. Iddrissu, S. M. Rowland, H. Zheng, Z. Lv, and R. Schurch, "Electrical tree growth and partial discharge in epoxy resin under combined AC and DC voltage waveforms," *IEEE Trans. Dielectr. Electr. Insul.*, vol. 25, no. 6, pp. 2183–2190, Dec. 2018.

[5] I. Kitani and K. Arii, "DC tree associated with space charge in PMMA," *IEEE Trans. Electr. Insul.*, vol. EI-22, no. 3, pp. 303–307, Jun. 1987.

[6] T. Tanaka and A. Greenwood, "Effects of charge injection and extraction on tree initiation in polyethylene," *IEEE Trans. Power App. Syst.*, vol. PAS-97, no. 5, pp. 1749–1759, Sep. 1978.

[7] N. Shimizu, H. Katsukawa, M. Kosaki, and K. Horii, "The space charge behavior and luminescence phenomena in polymers at 77K," in *Proc. IEEE Int. Conf. Electr. Insul.*, Philadelphia, PA, USA, Jun. 1978, pp. 1–4.

[8] S. S. Bamji, A. T. Bulinski, I. Powell, and N. Shimizu, "Light emission in XLPE subjected to HV in high vacuum and pressurized gas," *IEEE Trans. Dielectr. Electr. Insul.*, vol. 8, no. 2, pp. 233–238, Apr. 2001.

[9] X. Chen, D. Murdany, D. Liu, M. Andersson, S. M. Gubanski, U. W. Gedde, and Suwarno, "AC and DC pre-stressed electrical trees in LDPE and its aluminum oxide nanocomposites," *IEEE Trans. Dielectr. Electr. Insul.*, vol. 23, no. 3, pp. 1506–1514, Jun. 2016.

[10] M. Liu, Y. Liu, Y. Li, P. Zheng, and H. Rui, "Growth and partial discharge characteristics of electrical tree in XLPE under AC-DC composite voltage," *IEEE Trans. Dielectr. Electr. Insul.*, vol. 24, no. 4, pp. 2282–2290, Sep. 2017.

[11] Y. Liu and X. Cao, "Electrical tree growth characteristics in XLPE cable insulation under DC voltage conditions," *IEEE Trans. Dielectr. Electr. Insul.*, vol. 22, no. 6, pp. 3676–3684, Dec. 2015.

[12] F. Baudoin, S. Le Roy, G. Teyssedre, and C. Laurent, "Bipolar charge transport model with trapping and recombination: An analysis of the current versus applied electric field characteristic in steady state conditions," *J. Phys. D, Appl. Phys.*, vol. 41, no. 2, pp. 19–22, 2007.

[13] H. Liu, Y. Li, Y. Liu, M. Zhang, X. Xu, and A. Liu, "Electrical tree initiation properties in cross-linked polyethylene under DC-impulse composite voltages," *IEEE Access*, vol. 6, pp. 62890–62897, 2018.

[14] Y. Wang, F. Guo, J. Wu, and Y. Yin, "Effect of DC prestressing on periodic grounded DC tree in cross-linked polyethylene at different temperatures," *IEEE Access*, vol. 5, pp. 25876–25884, 2017.

[15] Y. Zhang, C. Alquie, and J. Lewiner, "Effect of the thickness of insulators on the build up of a space charge distribution," in *Proc. 8th Int. Symp. Electrets (ISE)*, Paris, France, Aug. 1994, pp. 928–933.

[16] Y. Li, T. Takada, H. Miyata, and T. Niwa, "Observation of charge behavior in multiply low-density polyethylene," *J. Appl. Phys.*, vol. 74, no. 4, pp. 2725–2730, Aug. 1993.

[17] G. Chen and J. Zhao, "Observation of negative differential mobility and charge packet in polyethylene," *J. Phys. D, Appl. Phys.*, vol. 44, no. 21, Jun. 2011, Art. no. 212001.

[18] J. M. Alison and R. M. Hill, "A model for bipolar charge transport, trapping and recombination in degassed crosslinked polyethene," *J. Phys. D, Appl. Phys.*, vol. 27, no. 6, pp. 1219–1299, 1994.

[19] H. C. Liu, X. B. Xu, and A. J. Liu, "Influence of DC pre-stress amplitude and time on initiation characteristics of grounded electrical tree in XLPE," (in Chinese), *Insulating Mater.*, vol. 52, no. 12, pp. 65–70, Dec. 2019.

[20] Y. P. Liu, H. C. Liu, and Z. G. Yang, "Effect of DC pre-stress on the induced characteristics of DC grounding electrical tree in XLPE," (in Chinese), *High Voltage Eng.*, vol. 43, no. 2, pp. 666–672, Jan. 2017.

[21] G. Bahder, T. Garrity, M. Sosnowski, R. Eaton, and C. Katz, "Physical model of electric aging and breakdown of extruded pplymeric insulated power cables," *IEEE Trans. Power App. Syst.*, vol. PAS-101, no. 6, pp. 1379–1390, Jun. 1982.

[22] M. Fukuzawa and M. Iwamoto, "Study of the relationship between space charge field and electrical treeing in low density polyethylene under a needle-plane electrode system," *Jpn. J. Appl. Phys.*, vol. 37, no. 7, pp. 4016–4020, 1998.
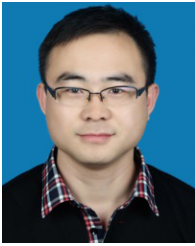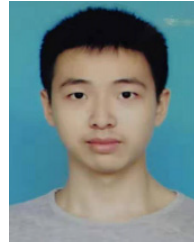
**HECHEN LIU** was born in Hebei, China, in 1989. He received the B.Eng. and Ph.D. degrees in electrical engineering from North China Electric Power University, Baoding, China, in 2012 and 2017, respectively. He is currently a Teacher with North China Electric Power University. His research interests include the insulation monitoring of power cable and the aging mechanism of high-voltage apparatus.

**SHAOXIN MENG** was born in China, in 1976. He works with the State Key Laboratory of Power Grid Environmental Protection, China Electric Power Research Institute, Wuhan. He is mainly engaged in power cable operation performance research, power system state detection technology, and evaluation technology research.
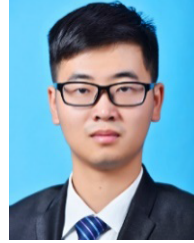
**XIAOBIN XU** was born in Hebei, China, in 1994. She received the B.Eng. degree in electrical engineering from North China Electric Power University, Baoding, China, in 2018, where she is currently pursuing the M.Eng. degree with the School of Electrical Engineering. Her research mainly focuses on the electric field and space charge distribution in HVDC cable insulation.

**ZHANPENG GUO** was born in Sichuan, China, in 1996. He received the B.Eng. degree in electrical engineering from North China Electric Power University, Baoding, China, in 2019, where he is currently pursuing the M.Eng. degree with the School of Electrical Engineering. His research mainly focuses on the aging characteristics of the HVDC cables and composite cross-arms.

**YUN-PENG LIU** (Member, IEEE) was born in Anhui, China, in 1976. He received the B.Eng. and Ph.D. degrees in electrical engineering from North China Electric Power University, Baoding, China, in 1999 and 2005, respectively. He is a Doctoral Supervisor and a Professor with North China Electric Power University. His research interests are UHV transmission, and the fault detection and diagnosis of electric equipment.

**MINGJIA ZHANG** was born in Zhejiang, China, in 1995. He received the B.Eng. degree in civil engineering from Northeast Electric Power University, Jilin, China, in 2017. He is currently pursuing the M.Eng. degree with the School of Electrical Engineering, North China Electric Power University. His research mainly focuses on the aging characteristics of the HVDC cables and composite cross-arms.

・・・